Published online 4 October 2007 *Nucleic Acids Research, 2007, Vol. 35, No. 20* ***6727–6739***
doi:10.1093/nar/gkm734

Human DNA mismatch repair: coupling of mismatch recognition to strand-specific excision

Huixian Wang and John B. Hays*

Department of Environmental and Molecular Toxicology, Oregon State University, Corvallis OR 97331-7301, USA

Received April 16, 2007; Revised August 23, 2007; Accepted September 4, 2007

ABSTRACT

Eukaryotic mismatch-repair (MMR) proteins MutSα and MutLα couple recognition of base mismatches to strand-specific excision, initiated *in vivo* at growing 3′ ends and 5′ Okazaki-fragment ends or, in human nuclear extracts, at nicks in exogenous circular substrates. We addressed five biochemical questions relevant to coupling models. Excision remained fully efficient at DNA:MutSα ratios of nearly 1 to 1 at various mismatch-nick distances, suggesting a requirement for only one MutSα molecule per substrate. As the mismatch-nick DNA contour distance *D* in exogenous substrates increased from 0.26 to 0.98 kbp, initiation of excision in extracts decreased as $D^{-0.43}$ rather than the D^{-1} to D^{-2} predicted by some translocation or diffusion models. Virtually all excision was along the shorter (3′–5′) nick-mismatch, even when the other (5′–3′) path was less than twice as long. These observations argue against stochastically directed translocating/diffusing recognition complexes. The failure of mismatched DNA in *trans* to provoke excision of separate nicked homoduplexes argues against one-stage (concerted) triggering of excision initiation by recognition complexes acting through space. However, proteins associated with gapped DNA did appear to compete in *trans* with those in *cis* to mismatch-associated proteins. Thus, as in *Escherichia coli*, eukaryotic MMR may involve distinct initial-activation and excision-path-commitment stages.

INTRODUCTION

Mismatch-repair (MMR) systems correct DNA replication errors and promote genomic stability in several other ways as well (1,2). MutS homodimer proteins in bacteria, or heterodimeric MSH2–MSH6 (MutSα) or MSH2–MSH3 (MutSβ) proteins in eukaryotes, bind specific base-mispairs or 'looped out' extra nucleotides in DNA. They then bind ATP and recruit bacterial MutL homodimers or eukaryotic MutLα (MLH1–PMS2) heterodimers into recognition complexes. Accessory proteins are used to create or identify specific strand ends for initiation of excision that proceeds through mismatches.

Biochemical studies using exogenous closed-circular substrates show that in *Escherichia coli* MutH proteins nick unmodified strands at hemi-methylated d(GATC) sites. This process, thought to mimic nascent-DNA identification *in vivo*, requires MutL and is stimulated by MutS and mismatched DNA (mmDNA). Subsequent loading of UvrD (MutU) helicase at the nick also requires mmDNA, MutS and MutL. To excise DNA from the nick towards the mismatch rather than away from it, *E. coli* uses 3′–5′ or 5′–3′ ssDNA exonucleases, as appropriate (3–5). The expected 3′ to 5′ travel of UvrD along continuous or nicked strands would expose 3′-ended or 5′-ended ssDNA, respectively. In biochemical experiments using exogenous circular substrates the excision-path-identification apparatus invariably chooses the shorter path from the nicked d(GATC) site to the mismatch.

In eukaryotes, excision during post-replication MMR is thought to initiate at nascent-DNA 3′ ends and perhaps 5′ Okazaki-fragment ends (1,2). Eukaryotes lack close analogs of the hemimethylated-GATC/MutH system, but in mammalian cell-free extracts mismatches in exogenous circular substrates efficiently provoke initiation of 3′–5′ or 5′–3′ excision at defined pre-existing nicks or gaps. No helicases have been implicated in eukaryotic MMR. MutSα–MutLα at mismatches is thought to interact with proteins already at strand discontinuities, such as the PCNA clamp and the clamp loader RFC. Other proteins may be recruited into pre-excision complexes. Despite the lack of a UvrD analog, active direction of (potentially bidirectional) eukaryotic MMR excision along the path towards the mismatch seems biologically desirable. Otherwise, mismatches might sometimes activate through space gratuitous excision of perfectly paired DNA in sister chromatids or adjacent Okazaki fragments. Indeed, eukaryotic MMR overwhelmingly directs excision along shorter nick-mismatch paths (typically 0.15–1 kbp), in 2–6 kbp circular exogenous substrates incubated in

*To whom correspondence should be addressed. Tel: +1 541 737 1777; Fax: +1 541 737 0497; Email: haysj@science.oregonstate.edu

cell-free extracts. (6–8) Since a wide variety of base-mispairs and extra-nucleotide loopouts preferentially provoke shorter-path excision (6,9), path selection seems unlikely to be determined by orientations of recognition complexes. Path selection mechanisms thus remain poorly understood.

To investigate how eukaryotes couple mismatch recognition to strand- and path-specific excision, we have focused here on mismatch-provoked excision of shorter nick-mismatch (3′–5′) paths in nicked circular exogenous substrates incubated in human nuclear extracts. This process is implicitly assumed to biochemically mimic excision initiated *in vivo* at 3′ ends of replicating DNA strands. Coupling specificity would seem to require at least (i) productive *interaction* of mismatch-recognition proteins (hMutSα•hMutLα, at a minimum) with nick-associated proteins such as PCNA and RFC and (ii) *commitment* to excision of the shorter nick-mismatch path. Figure 1 depicts three current models for the initial interaction process. Two models propose that recognition complexes move away from mismatches along DNA contours until they encounter nick-associated proteins. The third postulates that fixed recognition complexes contact nick-associated protein complexes through space, via DNA bending. Productive interactions between these complexes could immediately engender commitment to excision of the shorter nick-mismatch path: moving recognition complexes might automatically direct excision back along the path just traveled by the recognition complexes, or the intrinsic properties of through-space complexes between mismatch-bound and nick-associated proteins might dictate the path to be excised. However, analogy with the *E. coli* MutH-UvrD paradigm suggests that a *distinct second process* in eukaryotes might identify the shorter nick-mismatch path and commit to its excision.

Here we address five biochemical questions explicitly relevant to proposed mechanisms of commitment to mismatch-provoked shorter-path excision of nicked circular substrates in human nuclear extracts.

(1) At a minimum, how many hMutSα molecules per substrate are needed for fully efficient MMR?
(2) Can mismatch-provoked (processive) excision be initiated in both directions at nicks when one mismatch-nick path is not much longer than the other, as might be expected if hypothetical mobile recognition complexes stochastically chose their DNA-contour paths?
(3) How does the initial rate of commitment to excision depend on the mismatch-nick contour distance?
(4) Can a mismatch on one (non-nicked) substrate provoke in *trans* nick-initiated excision of a separate homoduplex substrate?
(5) Can proteins putatively bound to strand interruptions on a homoduplex substrate compete in *trans* with similar proteins bound at excision–initiation sites on separate substrates, themselves in *cis* to mismatches?

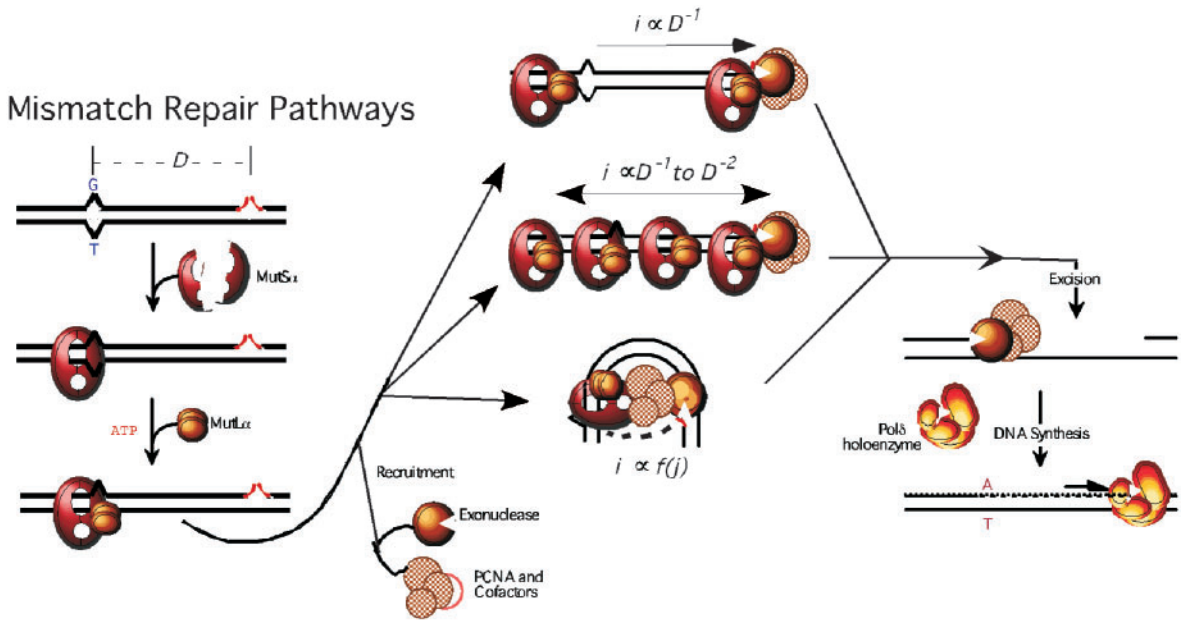

Figure 1. Alternative pathways for initial stage of mismatch repair in human nuclear extracts. A circular exogenous substrate, with (shorter-path) distance D from mismatch to nick, is represented linearly. Binding of MutSα and ATP-dependent recruitment of MutLα generate a ternary recognition complex at the mismatch. Concomitantly, a pre-excision complex—perhaps (an) exonuclease(s) plus accessory proteins such as PCNA and RFC—forms at the nick. Three alternative mechanisms for subsequent communication between recognition and pre-excision complexes are shown in the central section, with predicted dependencies of average-communication-time i on nick-mismatch distance D; upper central, communication by unilateral translocation along stochastically chosen paths from mismatch to nick (→), $i \propto D$; middle central, concentration-driven linear diffusion in both stochastically chosen directions from mismatch (↔), $i \propto D^2$ to $i \propto D$; lower central, communication through space by fixed recognition complex, coupling time related to the Jacobson–Stockmayer parameter j. The mechanism(s) by which communication between recognition and pre-excision complexes subsequently elicits commitment to excision are not specified.

We incubated circular DNA substrates (2–3 kbp) that contained base-mismatches and defined nicks in human nuclear extracts. We measured mismatch-provoked 3′–5′ excision and, in a few experiments, 5′–3′ excision. We used DNA substrates with mismatches separated from nicks by various contour distances, and varied substrate concentrations over a 12-fold range. Rates of commitment to mismatch-provoked excision remained constant even when DNA:hMutSα ratios approached 1 to 1. Excision-commitment rates only modestly decreased with mismatch-nick distance ($\propto D^{-0.43}$) as D increased from 0.26 to 0.98 kbp. Excision along the fixed 1.85-kbp longer path remained very low as the shorter path increased to 0.98 kbp. Mismatches on separate DNA molecules provoked no detectable excision of nicked homoduplex DNA in *trans*. However, gapped homoduplexes in only 6-fold excess interfered with excision of substrates in which nicks were in *cis* to mismatches. These findings, taken together, warrant close consideration of two-stage activation/commitment models for eukaryotic mismatch-provoked excision.

MATERIALS AND METHODS

Plasmids and substrates

In 'Substrate-Construction Details' section of Supplementary Data, we describe construction of plasmids pUC19MN100, pUCMN250, pUC19MN550 and pUC19MN1000, and their conversion into substrates sMN14, sMN26, sMN58 and sMN98, respectively, by replacing the DNA strands between the tandem sites for nicking endonuclease N. *Bst*NB I with oligomers creating G/T mismatches and nicking at the unique N. *Bbv*C IB sites. In these 1.9–2.8-kbp substrates, the 3′–5′ nick mismatch paths are 0.138, 0.259, 0.577 and 0.979 kbp, respectively; all 5′–3′ nick-mismatch paths are 1.85 kbp. Homoduplex substrates sMN14hmd, sMN26hmd, sMN58hmd and sMN98hmd were produced directly from the corresponding plasmids by nicking at N.*Bbv*C IB sites. To produce the non-nicked linear molecules L186MN14 and L186MN14hmd, we nicked substrates sMN14 and sMN14hmd with endonuclease N.*Bbv*C IA, 4 nt from the pre-existing N.*Bbv*C IB nicks on the opposite strands.

Mismatch correction and MMR excision

HeLa cells were purchased from the National Cell Culture Center, Minneapolis, MN. Nuclear extracts were prepared by a standard procedure (10). Briefly, proteins were extracted with 0.15 M salt from nuclei (released from cells broken by homogenization) and then precipitated with ammonium sulfate. Unless indicated otherwise, standard MMR mixtures contained, in 15 or 20 µl, 75 fmol of DNA (5.0 or 3.8 nM), 100 µg nuclear extract and 750 ng bovine serum albumin, plus the following components at the indicated concentrations: 20 mM Tris–HCL, pH 7.6; 1.5 mM ATP; 1 mM glutathione; 5 mM $MgCl_2$; 110 mM KCl. To measure excision, we incubated mixtures (without added dNTPs) at 37°C for indicated times, then mixed with 30 µl stop solution (25 mM EDTA, 0.67% sodium dodecyl sulfate, and 90 µg/ml proteinase K). DNA was extracted from reaction mixtures with phenol, precipitated and linearized with endonuclease *Ahd* I concominant with RNaseA treatment. To measure commitment to 3′–5′ excision DNA was annealed to radioactive oligomer 5′-GCTCACTCAAAG GCGGTAATACGGTTATCC (probe *A*), complementary to the continuous (sense) strand 20 to 49 nt from the N. *Bbv*C IB nicking site along the 3′–5′ path to the mismatch. Substrate-probe complexes were analyzed by electrophoresis and autoradiography and/or phosphoroimiaging. We used intensities of bands in ethidium-stained gels to normalize phosphoroimaging signals for DNA recovery.

To measure correction of (G/T) mismatches, MMR mixtures were supplemented with all four dNTPs to 100 µM. After isolation of product DNA as described earlier, samples were digested with *Ahd* I endonuclease, which linearizes all substrates, and with *Xho* I endonuclease, to detect correction of the G/T mismatch to G/C, before electrophoresis. Gels were stained with ethidium bromide and product and DNA band intensities measured using the Imagequant imaging and analysis system. Both of the above procedures have been described in detail (11,12). Purified MutLα (kind gift of Dr R. Michael Liskay, Oregon Health and Sciences University) was added where indicated. This preparation (13) complemented an extract of MLH1-deficient mouse embryonic fibroblasts for mismatch correction [Andrew Buermeyer (personal communication)].

Testing simulation of excision by mismatched DNA in *trans*

We tested the ability of linear (non-nicked) mismatched or homoduplex DNA, L186MN14 or substrates L186MN14hmd, to provoke excision of homoduplex sMN98hmd, as described earlier, except that in addition to probe *A* (20–49 nt down the 3′–5′ path), excision probes (*B*), (*C*) or (*D*), were used (separately). These oligomers are complementary to the nicked strand, respectively 59–87 nt, 482–510 nt or 965–993 nt along the 5′–3′ nick-mismatch path (see Figure 2 and Table 1).

Immunoassay of hMutSα in nuclear extracts

To detect hMSH6, and therefore hMutSα (MSH2–MSH6), in HeLa extracts we used an anti-MSH6 antibody from BD Pharmingen (cat. #G10919) with purified MutSα (kind gift of Dr Paul Modrich, Duke University; concentration previously determined by ultraviolet absorbance) as a standard. We separated extract proteins by electrophoresis in 10% polyacrylamide gels containing 0.1% sodium docecyl sulfate. We transferred bands to nitrocellulose membranes, and performed immunoassays by standard techniques, using ECL chemoluminescence reagents. Chemoluminescence signals for various levels of hMutSα standards were as follows: 150 ng, 52 780; 100 ng, 9554; 75 ng, 2964; 50 ng, 1142. The signal for 75 µg of HeLa nuclear extract was 3694; linear interpolation between the 75 ng and 100 ng standards yielded 94 ng MutSα. For a nuclear extract prepared from a second HeLa cell culture, the chemoluminescence signal was 95% of that for the first extract, assayed (again) at the same time. Assuming some loss in transfer, we estimate hMutSα

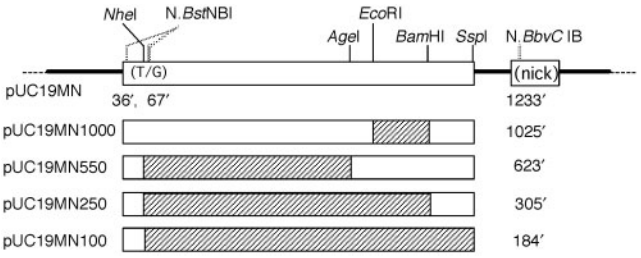

Figure 2. Construction of plasmids for generation of MMR substrates. See 'Plasmids and substrates' section for details. The solid dark line represents DNA from (circular) 2-kbp plasmid pUC19Y and empty rectangles show inserted DNA, from plasmid pCYFP + 1 and various synthetic linkers. Diagonally slashed boxes show DNA removed by cutting at restriction endonuclease sites (*Nhe*I, *Age*I, *Eco*RI, *Bam*HI, *Ssp*I) indicated by solid vertical lines, and joining via short synthetic linkers. The tandem N.*Bst*NBI nicking sites indicated by dotted vertical lines, used to generate gaps for insertion of mismatch-creating 31-nt oligomers, are at coordinates 36′ and 67′ in all plasmids. The coordinates of the N.*Bbv*CIB sites used to generate excision–initiation nicks in substrates reflect the alterations in the nick-mismatch 3′–5′ paths.

Table 1. Comparisons of 3′–5′ and 5′–3′ excision

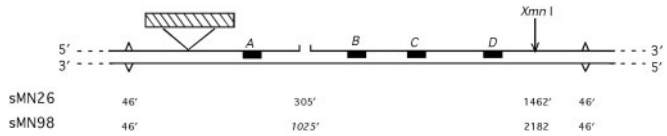

Substrate[a]	Relative excision (%) detected by indicated probes 3′–5′ path 5′–3′ (longer) path[b]			Relative (%) 3′–5′ excision initiation rate[c]	
	[*A*]	[*B*]	[*C*]	[*D*]	
sMN26hmd	0.6	9	0.2	0.1	
sMN26	(100)	77	8.9	1.9	(100)
sMN98hmd	0.5	18	0.3	0.2	
sMN98	59	84	10.8	2.4	43
L2182sMN98hmd		18		0.6	$\ll 0.5$[d]
L2182sMN98		77		1	29
L1462sMN26					103

Upper diagram shows relative positions (not to scale) of nicks (coordinates 305', 1025'), mismatches (coordinate 46') and excision probes *A*, *B*, *C* and *D* (collinear with nicked strands), in (circular) sMN26 and sMN98 substrates. Shaded rectangle denotes additional DNA in sMN98 (Figure 6). The diagram repeats the mismatch positions. Coordinates of probes *A*, *B*, *C* and *D*, respectively are 256′–285′, 364′–392′, 787′–815′, and 1270′–1298′ for sMN26, and 976′–1005′, 1084′–1112′, 1507′–1535′, and 1990′–2018′ for sMN98.

[a]sMN26hmd, sMN98hmd and L2182sMN98hmd contain no mismatches. Cleavage of sMN26 and sMN98 by endonuclease *Xmn*I at coordinates 1462 and 2182, respectively, yields linear substrates L1462sMN26 and L2182sMN98.

[b]Excision signals determined after 4 min incubation by gel electrophoresis, and phosphorimaging as described in Figure. 3 legend and under 'Materials and Methods, *Mismatch correction and MMR section excision*'. Specific radioactivities of the various probes were adjusted to be approximately equal and binding of probes to ssDNA at the various sites is assumed to be similarly efficient.

[c]Rates derived fom slopes generated from excision signals measured at 1, 2, 3 and 4 min, except L2182sMN98 excision was measured for 4 min only.

[d]The low background signals for apparent homoduplex excision do not show consistent time courses. Rates thus cannot be meaningfully determined, but would be much less than the 4 min signal (0.5%).

levels in our MMR reactions to be ~500 fmol per 100 μg extract protein, in good agreement with the 580 fmol measured by Modrich and coworkers (14,15); 580 fmol correspond to 33 nM in standard 15 μl MMR reaction mixtures.

RESULTS

Experimental system

We constructed 2–3-kbp circular MMR substrates sMN14, sMN26, sMN58 and sMN98, in which 3′–5′ excision paths from pre-existing nicks to (G/T) mismatches were 0.14, 0.26, 0.58 and 0.98 kbp, respectively (Figure 2; see under 'Materials and Methods' section, Plasmids and Substrates and 'Substrate Construction Details' of Supplementary Data). Mismatches and nicks were in the same DNA-sequence contexts, respectively, in these substrates. The human (HeLa-cell) nuclear extracts routinely employed appear contain all proteins needed for efficient and specific MMR, apparently as active as purified recombinant proteins, if not more so. We and others have previously demonstrated rapid time courses, high yields and high specificities, for both MMR excision and mismatch correction in these extracts (6,7,9). Here we assayed commitment to 3′–5′ excision (in the absence of exogenous dNTPs) as appearance of ssDNA that was bound by an oligonucleotide probe about 40 nt down the path from the nick, as described (9). We previously showed this excision assay to be over 100 to 1 specific for nicked versus continuous strands, over 20 to 1 specific for shorter versus longer nick-mismatch paths and highly specific for mismatched versus homoduplex DNA (7–9,16). We measured correction of a G/T mismatch as restoration of a cutting site for *Xho*I endonuclease. Figure 3 shows that, as previously, excision–commitment time courses were linear for at least 4 min and preceded parallel mismatch–correction time courses.

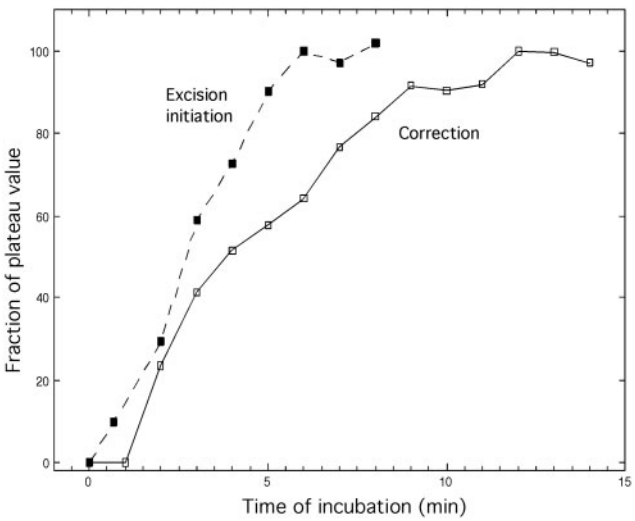

Figure 3. MMR excision–initiation and mismatch–correction time-courses. Initiation of 3′–5′ excision (filled squares) and correction (open squares) of (G/T) substrate sMN26 (5 nM) were assayed at indicated times as described under 'Mismatch correction and MMR excision' section. Correction yield (relative to input substrate) was 55%.

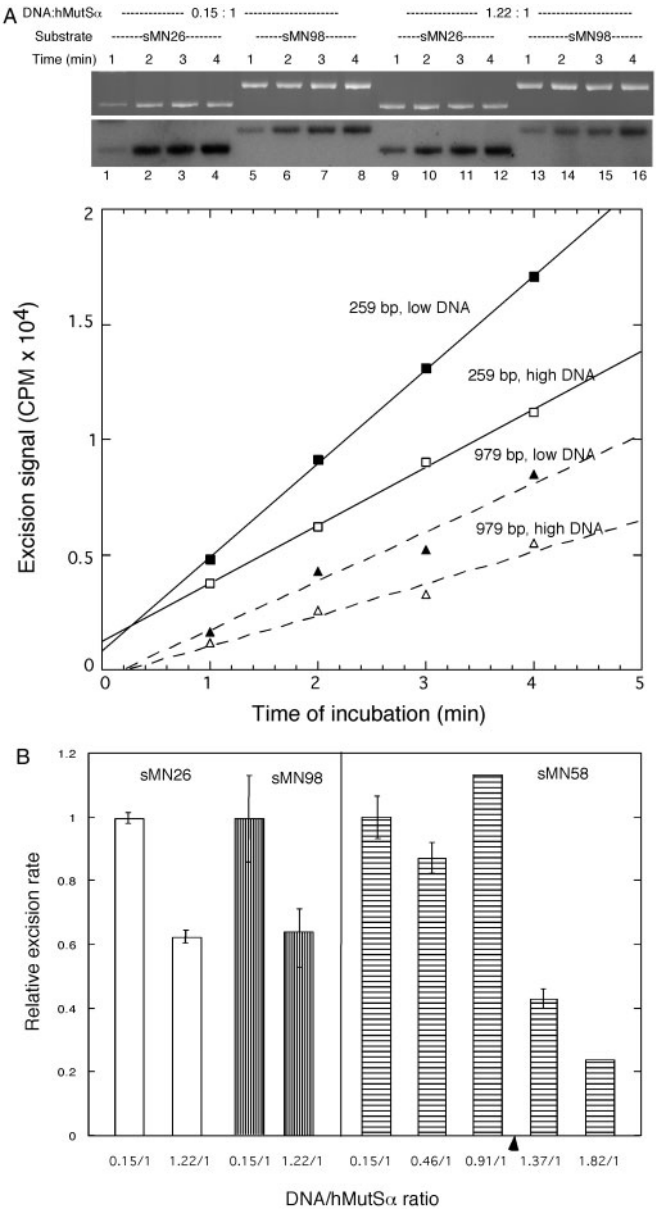

Figure 4. Dependence of MMR excision–initiation rates on DNA-substrate concentration (**A**) Excision time-course for substrates sMN26 and sMN98 at low and high concentrations. Initiation of 3′–5′ excision of (G/T) substrates sMN26 and sMN98 at 3.8 nM (low DNA) or 30 nM concentrations (high DNA) was assayed using probe *A* as described under 'Mismatch correction and MMR excision' section, except that the volume of the high-DNA reaction mixture loaded onto the gel was reduced so as to electrophorese equal amounts of DNA from each reaction. hMutSα concentration was ~25 nM ('Immunoassay of hMutSα in nuclear extracts' section). hMutLα concentrations were increased from the 8 nM reported by Genschel and Modrich (14) to 30 nM, by addition of purified protein. Upper panels; ethidium-stained gels and phosphorimages for substrates sMN26 and sMN98 for indicated substrate:hMutSα ratios and incubation times. Lower panel: plotted excision values and fitted slopes for sMN26 (squares) at 0.15/1 (filled squares) and 1.22/1 (open squares) DNA:hMutSα ratios and sMN98 (triangles) at 0.15/1 (filled triangles) and 1.22/1 (open triangles). Another trial yielded very similar results. (**B**) Left-hand panel. Excision of substrate sMN58 at a series of DNA:hMutSα ratios. The single trial was performed as described earlier, except sMN58 concentrations were 3.8, 11.4, 22.8, 34.2 and 45.6 nM and hMutSα concentration was 25 nM (estimated by immunoassay), hMutLα was supplemented to roughly 70 nM protein, and excision was measured at only two or three time points. Equal amounts of DNA from each reaction were electrophoresed. Relative excision rates for indicated sMN58: hMutSα ratios (horizontally lined bar) are relative to rate for 0.15 to 1 ratio. Arrow indicates 1 to 1 position. Right-hand panel. Rates for sMN26 (empty bars) and sMN98 (vertically lined bar) [see (**A**) earlier] at DNA: hMutSα ratio 1.22 to 1, relative to rate at 0.15 to 1. Error bars show 95% confidence limits for fits of slopes through four or three points. A duplicate experiment yielded highly similar results.

In the 'Validation of Excision Assay' section of Supplementary Data, we show that initial excision rates and initial correction rates decreased in parallel when the mismatch-nick contour distance increased from 0.26 to 0.98 kbp; excision thus appears to be rate-limiting (Figure 3S). The increase in excision–correction lag time corresponds to an excision progress rate of 4–7 nt/s, in agreement with 5 nt/s previously estimated by assaying excision at two different positions in the same substrate (7).

In the 'Validation of Excision Assay' section of Supplementary Data, we show excision to be 200-fold specific for mismatched versus homoduplex substrates (Figure 1S), and describe use of an alternative excision assay (Figure 2S) to demonstrate equality of plateau excision and correction yields—both roughly 45–55% of input substrate. This is consistent with our previous demonstration that excised intermediates could be quantitatively converted to corrected products (9). We also summarize eight independent lines of evidence, including previous work (7,8,17) and findings here, that validate the assumption that our assays measure 3′–5′ (shorter-path) excision that initiates at pre-existing nicks and proceeds towards mismatches ('Evidence for 3′–5′ Rather than 5′–3′ Excision' section in Supplementary Data). Thus, any 5′–3′ excision from MutLα-induced incisions [near mismatches but outside the shorter (3′–5′) paths from pre-existing nicks to mismatches], previously seen in reconstituted systems (18), seems not to be substantial in these nuclear extracts; see also under 'Discussion' section.

Dependence of excision–commitment and mismatch–correction efficiencies on MutSα-substrate stoichiometry

To estimate the minimum number of hMutSα heterodimers needed for efficient MMR, we first measured commitment of mismatch-provoked excision to the shorter 3' nick-mismatch paths in substrates sMN26 and sMN98, using DNA-substrate concentrations of 3.8 and 30 nM in each case (Figure 4A). MutSα was measured to be 25–30 nM by immunoassay of HeLa nuclear extracts and hMutLα was increased from the estimated endogenous 8 nM (14) to a nominal 30 nM using purified recombinant hMutLα, to ensure that MutSα was limiting. Figure 4B (left) shows excision–initiation rates (slopes from Figure 4A) at DNA:MutSα ratios of 0.15 to 1 and 1.2 to 1, for mismatch-nick distances of 0.26 and 0.98 kbp. Excision of both substrates was reduced by only 37% when DNA:hMutSα ratios increased. Therefore, longer distances did not require more MutSα, contrary to expectations if multiple loadings were needed to drive linearly diffusing MutSα–MutLα complexes to nicks.

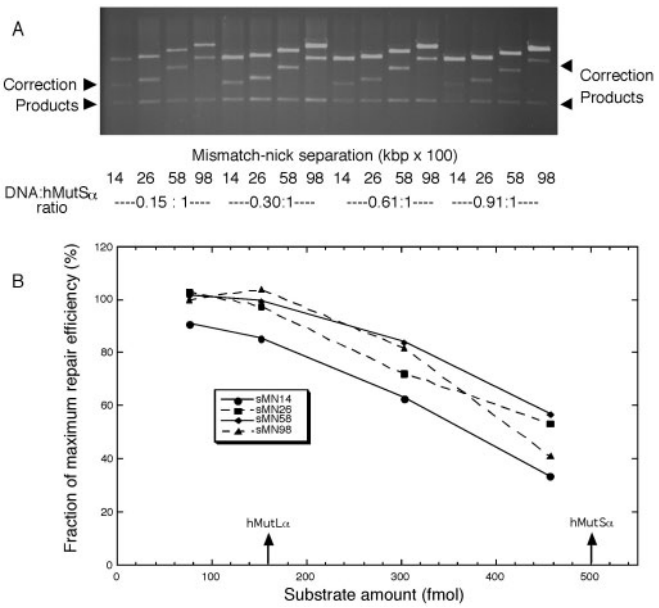

Figure 5. Mismatch correction at increasing DNA:protein ratios. Analysis of correction after 30 min. (G/T) of substrates sMN14 (filled circles), sMN26 (filled squares), sMN58 (filled diamonds) and sMN98 (filled triangles), at the indicated concentrations, was as described under 'Mismatch correction and MMR excision' section. Upper panel: ethidium-stained electropherograms. Arrows indicate corrected-product bands expected for substrates sMN14 (left) and sMN98 (right). Lower panel: plot of correction efficiency relative to that for 75 fmol of substrate sMN98 (55% absolute product yield). Arrows indicate immunoassayed concentration of hMutSα in HeLa nuclear extracts and reported concentration for MutLα (14).

Similarly, commitment to excision of substrate sMN58, measured at a series of increasing DNA: hMutSα ratios (Figure 4B, right), remained constant until the ratio approached 1 to 1 (arrow), then decreased markedly. If this decrease to some extent reflected sub-optimal levels of other proteins, this experiment might actually overestimate MutSα requirements. Furthermore, although MSH6 detected by the antibody is probably bound to MSH2 (19), not all MutSα heterodimers may be active, even in nuclear extracts. On the other hand, the hMutSα immunoassay depends indirectly on the absolute accuracy of measured concentrations of hMutSα protein standards and on similar binding of the (monoclonal) antibody to recombinant MSH6 and to MSH6 from extracts Within the limits of these uncertainties then, rates of commitment to 3′ excision were the same whether there were seven or approximately one hMutSα heterodimer per substrate.

To determine whether 1–2 hMutSα proteins per substrate sufficed for mismatch correction as well, we incubated increasing concentrations of substrates in HeLa-extract MMR-reaction mixtures containing dNTPs (Figure 5). Correction efficiencies decreased, albeit modestly, when substrate concentrations exceeded expected MutLα concentrations. Therefore MutLα and/or some other component(s), perhaps required for DNA resynthesis, might be rate-limiting. At a DNA:hMutSα of 0.91 to 1 mismatch correction was only 40–60% less than correction at 0.15 to 1, with no systematic variation with mismatch-nick separation. We cannot rule out turnover of MMR proteins during the 30-min incubation, but ligation of nicks in extracts (6,9) would most likely limit initiation after 3–5 min. Mismatch–correction stoichiometries (Figure 5) thus appear consistent with the roughly 1 to 1 excision–commitment stoichiometries (Figure 4).

Dependence of excision initiation on mismatch-nick DNA-contour distance

We compared excision–initiation rates for shorter-path (3′–5′) distances (D) of 0.14, 0.26, 0.58 and 0.98 kbp (but constant 5′–3′ distances of 1.85 kbp). Figure 6A shows excision commitment to increase linearly during at least the first 4 min, and Figure 6B (upper half) shows a log–log plot of initial rates versus mismatch-nick distances, for three independent trials. [In these and other MMR excision experiments (16) experimental variation using substrate sMN14 was greater than that using other substrates (standard deviations twice those using sMN26, sMN58 or sMN98). We do not speculate on reasons for this here. We dropped the sMN14 data from the analysis shown in Figure 6A, and did not use sMN14 in subsequent experiments.] The mean of the slopes of the experimental lines (Figure 6A, upper half) is 0.43 ± 0.04 (SD). Numerically similar differences in excision time courses were obtained for substrates sMN26 and sMN98 when excision was assayed as formation of ssDNA tracts resistant to endonuclease *Ssp* I ('Validation of Excision Assay' in Supplementary Data; Figure 2S and data not shown). These data are in good agreement with the 1.6 to 1.8 times higher initial rates of excision and correction of substrate sMN26 versus sMN98 seen in Figure 4 and Figure 3S, since (0.98/0.26) 0.43 = 1.77.

Testing for competition between shorter-path (3′–5′) and longer-path (5′–3′) MMR excision

In some MMR models, MutSα–MutLα complexes are hypothesized to slide from mismatches toward nicks along DNA contours and directly trigger excision back along the paths just traversed as soon as they productively interact with nick-associated proteins. Thus, the first-arriving MutSα–MutLα would determine the direction of excision. Even if hypothetical multiple recognition complexes stochastically chose their sliding directions, so roughly equal numbers set out along both mismatch-nick paths in circular substrates, excision initiation would be biased towards the shorter path. This bias is indeed observed when one path is much longer than the other. However, as the lengths of shorter and longer paths became more nearly equal, a recognition complex traveling the longer path should occasionally arrive first and direct excision back along the longer path, pre-empting shorter-path excision. Here, such increased (5′–3′) excision of the 1.85-kbp longer-path as the shorter-path contour distance D increased might account for the observed decrease in shorter-path excision as $D^{-0.43}$ (Figure 6B). To test for this possibility, we compared the initial rates of commitment to nick-initiated 3′–5′ and 5′–3′ excision of substrates sMN26 and sMN98, in which the 5′–3′ path was 7.2 or 1.9 times as long as the 3′–5′ path, respectively.

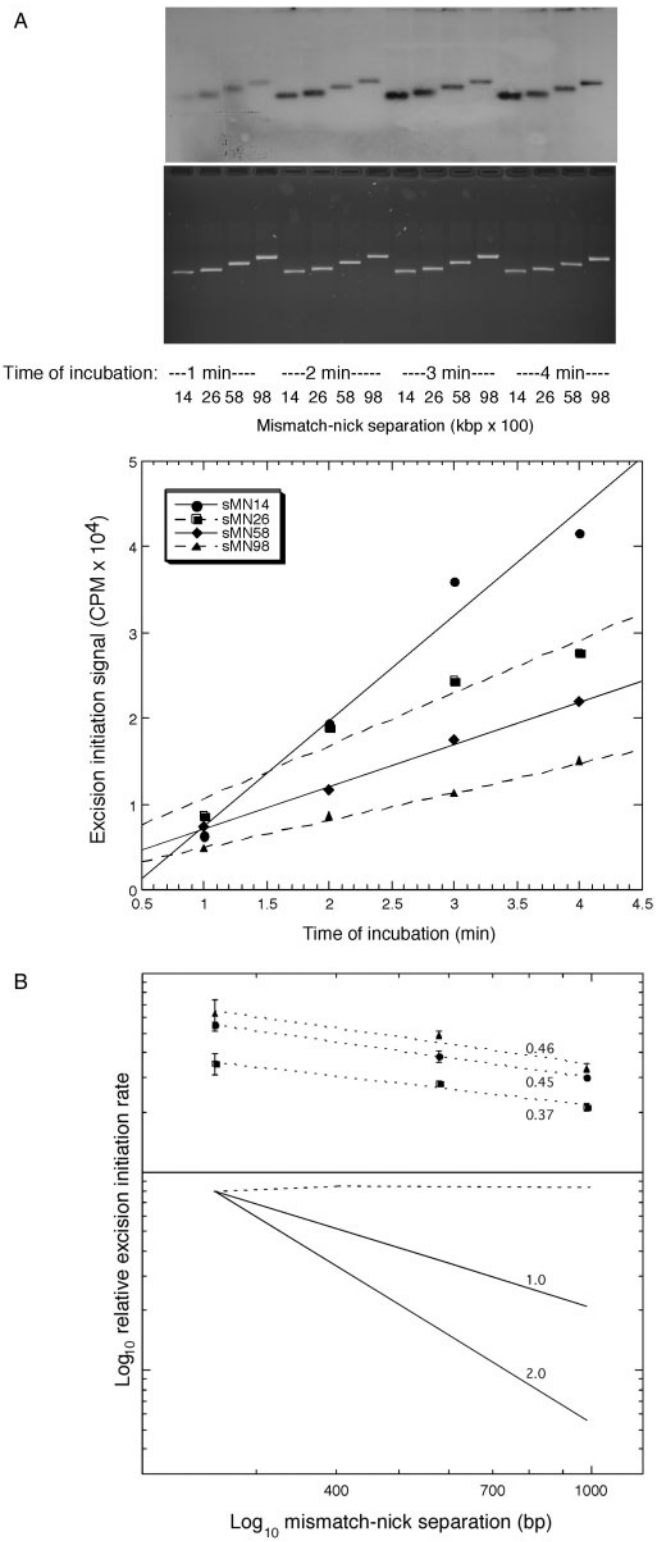

Figure 6. MMR excision in substrates with different mismatch-nick separations. (**A**) Time courses. Initiation of 3′–5′ excision of 5 nM (G/T) substrates sMN14 (filled circles), sMN26 (filled squares), sMN58 (filled diamonds) and sMN98 (filled triangles) was assayed using probe *A*, as described under 'Mismatch correction and MMR excision' section. Upper panel: autoradiograph of bound excision probes. Middle panel: ethidium staining of total DNA. Lower panel: phosphoroimager-measured excision signals normalized for total DNA recoveries, with least-squares slopes shown. Where excision signals at 3 min appear to exceed those at 4 min, DNA recoveries were correspondingly higher. (**B**) Distance dependence of rates of excision initiation. Complete sets of excision analyses (four substrates, four time points) were obtained in three separate trials. For each trial, differences in excision-probe intensity and phosphorimaging time introduced different (constant) scaling factors into the different sets of signals. Thus, even if absolute rates (moles of excised product per min) for any particular substrate were identical, the scaling factors would cause the observed rates (phosphorimager signal per minute) to be different. In order to compare rates among the three trials, we determined the standardization factors needed to make equal the excision signals for the same single reference point in each trial, arbitrarily chosen as the 1-min excision signal for substrate sMN26, then scaled all other points in each trial using the respective standardization factor. Upper half: Log–log plot of excision–initiation rates time-point slopes for each substrate against mismatch-nick distance. Error bars indicate 95% confidence limits for fits of slopes to standardized time points, except where less than sizes of points. Rates (excision signal per minute) for the trial in Figure 5A (lowest panel), and for two similar trials, were each multiplied by arbitrary factors to position them conveniently on the plot. Since the parameter of interest is the log (rate) versus log (separation) slope, the actual values of this constant factor (and the standardization factors described earlier) are irrelevant. The rates determined by the standardized excision signals varied slightly in the separate trials. However, the slopes (dotted lines) corresponding to the distance dependence of the excision–initiation rates were similar (0.46, 0.45, 0.37). Lower panel: theoretical curves corresponding to variation in initiation rate with mismatch-nick distance as D^{-1} or D^{-2} (solid lines), or as the Jacobson–Stockmayer cyclization parameter *j* for chain lengths of 0.3–1 kbp [Supplementary Data 5, 6; Figure 4S; ref. (25)].

Table 1 shows excision rates expressed relative to the rate measured 40 nt down the 3′–5′ (shorter) nick-mismatch path (probe *A*) in sMN26. Increasing the 3′–5′ path from 0.26 kbp (sMN26) to 0.98 kbp (sMN98) decreased the rate of 3′–5′excision (probe *A*) 1.7-fold, in further support of the $D^{-0.43}$ dependence observed in several other experiments (see earlier). We assayed for putative mismatch-specific 5′–3′ excision 980 nt down the (1895 nt) 5′–3′ nick-mismatch paths (probe *D*) in sMN26 and sMN98, because of the high non-specific (but non-processive) 5′–3′ excision typically initiated at nicks (9,14,20); note the high 5′–3′ excision of homoduplex sMN26hmd and sMN98hmd measured 70 and 500 nt down the nick-mismatch path (probes *B* and *C*). Here relative probe-*D* signals (1.9 and 2.4%, respectively) for sMN26 and SMN98 only slightly exceeded the 0.1–0.2% background for nicked homoduplex substrates sMN26hmd and sMN98hmd. Thus, the ratio for 3′–5′ versus 5′–3′ mismatch-provoked processive excision of sMN98 was at least 30/1, even when the path ratio was only 1/1.85. (We previously explained high non-processive 5′–3′ longer-path excision in mismatched substrates in terms of gaps (better initiation sites for hEXOI) opened up by mismatch-provoked 3′–5′ (shorter-path) excision.] Also, linearized substrates L2182sMN26 and L2182sMN98, whose longer (5′–3′) nick-mismatch paths were broken by *Xmn*I endonuclease cleavage, showed no increases in rates of 3′–5′ excision commitment (Table 1, column 6). This rules out non-productive sequestration of the excision apparatus by hypothetical complexes that arrived at nicks via 5′–3′ mismatch-nick paths but were themselves unable to provoke processive 5′–3′ excision.

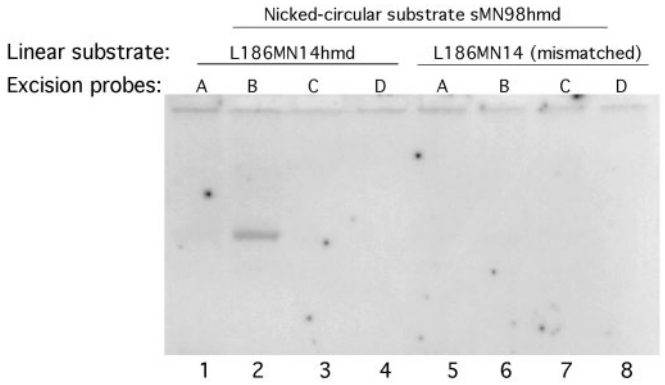

Figure 7. Testing for excision provoked by mismatched DNA in *trans*. Analysis of excision after 4 min at specific sites in (G/T) substrate sMN98 (30 nM) in the presence of (non-nicked) linear homoduplex L186MN14hmd (30 nM) or mismatched L186MN14 (30 nM) and the positions of the indicated probes (collinear with the nicked strand) were as described under 'Testing simulation of excision by mismatched DNA in *trans*' section. Probe *A* measures excision of the nicked strand 40 nt down the 3′–5′ path. Probes *B*, *C*, *D* measure excision of the nicked strand 50, 500 and 1000 nt, respectively down the 5′–3′ path. Probe positions are shown schematically at the top of Table 1. Only 1/8 of reaction volumes were loaded onto gels.

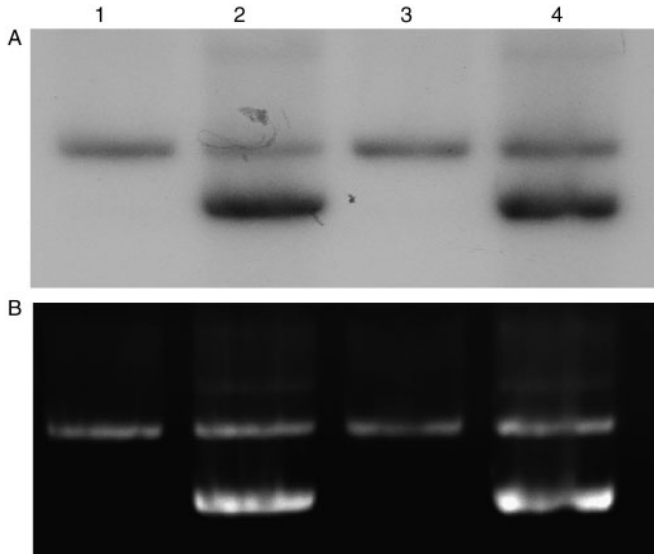

Figure 8. Testing for inhibition of MMR in trans by gapped DNA. Standard MMR reaction mixtures (15 µl) contained 5 nM (G/T) nicked substrate sMN98 and 30 nM gapped (homoduplex) plasmid pUCMN100 (precursor of substrate sMN14) containing a 32-nt gap, where the mismatch-creating oligomer was subsequently inserted; (see 'Materials and Methods, Construction of Plasmids and Substrates' section in Supplementary Data) mixtures were assembled in two different ways: (i) sMN98 alone (lane 1) or sMN98 plus gapped pUC19MN100 DNA (lane 2) were mixed with MMR buffer before addition of nuclear extract; (ii) extract protein was incubated in MMR Buffer without (lane 3) or with (lane 4) gapped pUC19MN100 for 30 sec. at 37°C before addition of sMN98. In both cases reactions were continued for 4 min at 37°C. Standard excision–commitment assays employed binding of Probe *A* (Table 1), electrophoresis, quantitation of DNA loaded by ethidium bromide staining (lower panel) and phosphorimaging (upper panel). Lane 3 was appreciably underloaded. Note that probe *A* binds to ssDNA produced at the same sites in sMN98 by mismatch-provoked 3′–5′ excision (lanes 1–4) or in gapped pUC19MN100 by non-specific 5′–3′ excision (lanes 2 and 4).

These observations suggest that either hypothetical moving recognition complexes are directed to move away from mismatches exclusively along shorter mismatch-nick paths (even when only 45% shorter than longer paths), or that some other mechanism(s) determine the paths for mismatch-provoked excision.

Testing for interactions between MMR-associated proteins on different substrates

The experiments described earlier, taken together, argue strongly against the first two coupling models illustrated in Figure 1, where recognition complexes stochastically choose paths to diffuse/translocate from mismatches to nicks, then automatically direct excision back along the paths just traveled. We performed two experiments to challenge the third model shown in Figure 1—activation of excision via interaction through space of recognition proteins at mismatches with proteins loaded at nicks, such as PCNA and RFC (Figure 1). First, we tested the ability of (G/T) mismatches on non-nicked (linear) substrate L186MN14g/t to in *trans* provoke excision of nicked (circular) homoduplex sMN98hmd (Figure 7), as assayed at various sites (probes *A*–*D*; see Table 1). Mismatched L186MN14g/t provoked no detectable 3′–5′ excision (probe *A*) or processive 5′–3′ excision (probe *D*) of sMN98hmd, when both substrates were 30 nM (Figure 7) or 15 nM (not shown). Surprisingly, there was no non-specific 5′–3′ excision (probe *B*) of sMN98hmd when mismatched L186MN14g/t was in *trans* (lane 6), even though this excision was substantial when homoduplex L186MN14hmd was in *trans* (lane 2). This suggests that hEXOI might be sequestered by hMutSα–hMutLα complexes at mismatches, at least under conditions where shorter-path (3′–5′) excision was not initiated.

In a second challenge to through-space models for recognition-excision coupling, we asked whether PCNA and associated proteins loaded at shorter (32 nt) gaps on homoduplexes might compete in *trans* with the same proteins loaded at nicks in *cis* to mismatches. We assembled standard MMR reaction mixtures containing only 5 nM substrate sMN98 (Figure 8, lanes 1 and 3) or 5 nM sMN98 plus excess (30 nM) gapped plasmid pUCMN100 (lanes 2 and 4) in two different ways. Commitment to 3′–5′ shorter-path excision of sMN98 after 4 min was then measured by the standard assay, using probe *A*. (The 32-nt gap in pUCMN100 is at the position where a (G/T) mismatch was present in sMN14. Since non-specific 5′–3′ excision initiated at the gap in pUCMN100 would also produce ssDNA at the site bound by probe *A*, probe-binding signals (Figure 8, upper panel) appear at the positions of substrates sMN98 (lanes 1–4) and pUC19MN100 (lanes 2 and 4).] Excess (30 nM) gapped plasmid in *trans* inhibited mismatch-provoked 3′–5′ excision by 40% (Figure 8, lanes 1 versus 2) or 27% (lanes 3 versus 4). (The ethidium-bromide-stained electropherograms (Figure 8, lower panel) show lane 3 to be appreciably underloaded relative to other lanes.]

It seems unlikely that all inhibition was actually due to titration by gapped plasmids of one or more accessory proteins needed for MMR–PCNA, RFC, EXOI or RPA (10), thus making them unavailable to the (G/T) substrate sMN98. The concentration of the two DNA substrates *together* (35 nM) is less than the protein concentrations expected for 100 μg HeLa extract in a 15 μl volume: 50 nM PCNA, 40 nM RFC and 100 nM RPA (21). hEXOI is expected to be only 5 nM in extracts. However, in the previous experiment (Figure 7), ExoI appeared to be bound well by 5 nM mismatched DNA (L186MN14g/t), but not by homoduplex DNA (L186MN14hmd). Furthermore, RPA is in substantial (3-fold) molar excess over gapped DNA. Genschel and Modrich (14) previously showed that hRPA binding to gaps protected them against hEXOI excision, presumably by inhibiting hEXOI. Thus, most hEXOI should here be associated with the mismatched test substrate, for two reasons. Furthermore, in another experiment (data not shown) we analyzed excision of 3.8 nM test substrate in the presence of 22.5 nM gapped competitor plasmid in HeLa extracts supplemented with recombinant hPCNA (from M. O'Donnell; 100 nM), yeast RFC [100 nM; highly active in reconstituted human MMR (10)], and hRPA (from M. Goodman; 180 nM), after which recombinant hEXOI (from Guo-Min Li; 75 nM) was added. The added excess hEXOI dramatically increased non-specific 5′–3′ digestion of the gapped competitor plasmid, despite the prior incubation with proteins that might be expected to protect the gap. Because background DNA was now present throughout the electrophoresis gels we could not quantitatively assay excision of the test substrate. However, even in the presence of excess hPCNA, yRFC, hEXOI and hRPA, gapped plasmid appeared to again inhibit this excision, by (very roughly) 20%. In the absence of added protein, inhibition was now measured to be 22%. The data of Figure 8 might be explained in more than one way, and we cannot rule out titration of some unknown rate-limiting protein by 30 nM pUCMN100. However, this experiment did not falsify models in which initial through-space interactions initiate the coupling process.

DISCUSSION

We have addressed five biochemical questions directly relevant to current models for MMR recognition–excision coupling in human nuclear extracts. We analyzed initial rates of mismatch-provoked commitment to 3′–5′ excision along the shorter paths between defined nicks and base mismatches in exogenous circular substrates, with the following results. (I) One or two hMSH2–MSH6 (hMutSα) mismatch-recognition proteins per DNA substrate appeared fully sufficient. (II) Mismatch-provoked (processive) 5′–3′ excision along the longer nick-mismatch path was much lower than 3′–5′ shorter-path excision, even when the 5′–3′ path was only 55% longer. (III) The initial rate of shorter-path excision decreased with the mismatch-nick contour distance D as the –0.43 (±0.04) power. (IV) Mismatches on one DNA molecule provoked in *trans* no detectable initiation of excision at nicks on separate homoduplex DNA molecules. (V) However, excess gapped homoduplex DNA, presumably associated with PCNA and RFC proteins, substantially inhibited in *trans* the excision initiated at nicks in *cis* to the mismatches, in three independent experiments.

Below we analyze alternative interpretations of our observations in terms of the recognition–excision coupling mechanisms shown in Figure 1 and other models. First however, the possibility that our experiments do not actually measure 3′–5′ excision needs to be addressed. Modrich and coworkers (18) recently reconstituted with several purified proteins a system in which hMutLα incised DNA in circular (6 kbp) substrates. Incisions were widely distributed around the substrate, but were somewhat more likely near the mismatches but outside (5′ to) the 0.14 kbp 3′–5′ path from the pre-existing nick to the mismatch. Incisions made in nuclear extracts were more tightly focused there. Addition of human exonuclease I (hEXOI) engendered 5′–3′ excision from the hMutLα-induced incisions. Could the excision that we measure 40 nt down the 3′–5′ path from the pre-existing nick to the mismatch actually reflect 5′–3′ excision from MutLα incision, through the mismatch and back to the pre-existing nicks in the various substrates, as the Modrich studies might suggest? This appears inconsistent with several observations here and previously. (i) Time courses of excision measured at sites farther down 3′–5′ paths from pre-existing nicks to mismatches were parallel to, but lagged, time courses of excision only 40 nt from nicks [(7): see also our analysis of Figure 2S here]. (ii) Rates of excision at the beginning of 3′–5′ nick-mismatch paths were not affected by downstream blockades, but excision was negligible beyond (5′ to) blockades (8,17). (iii) Initial rates of commitment to excision in nuclear extracts are the same at DNA:hEXOI ratios of 1 to 1 and 7 to 1 (Figure 4). Under 'Validation of Excision Assay' section of Supplementary Data, we discuss in more detail these and five other independent lines of evidence. Taken together, they suggest that in complex nuclear extracts (at least when hEXOI is not in excess over DNA substrate), most mismatch-provoked excision initiates at pre-existing nicks and proceeds 3′–5′ along shorter paths towards mismatches. Below we discuss alternative interpretations of findings *I–V*.

(I) *DNA:MutSα stoichiometry*. Efficient correction of mismatches in a reconstituted system was reported to require roughly four recombinant hMutSα molecules per DNA substrate (22). However, recombinant proteins purified from insect cells (including hMutSα and MutLα) are frequently less active than proteins purified from extracts, themselves not necessarily as active as endogenous proteins in the extracts. Without independent assays, recombinant hMutSα cannot be assumed to be fully active. Interestingly, fewer hMutSβ molecules per substrate appeared sufficient for correction of a 2-nt extrahelical loopout in the same previous study. Previous quantitative immunoassays (14,15) of MutSα in nuclear extracts, combined with our data (Figures 4 and 5), indicate that one to two hMutSα molecules suffice for efficient MMR.

An alternative explanation for our stoichiometry result might be rapid formation of multiple MutSα–MutLα complexes that then very rapidly slide towards mismatches and activate excision, or rapidly dissociate into solution and load again. Thus, if multiple rounds of loading, sliding and dissociation occupied only a very few seconds, MMR excision at 1 to 1 MutSα:DNA ratios might appear to be as rapid as at 7 to 1, as was observed.

The detailed discussion of this alternative explanation in 'Supplementary Information, Alternative Interpretations of Measurements for hMutSα:DNA Stoichometry and Excision Rates versus Nick-Mismatch Distance' is summarized later. Central to this alternative is a requirement for very rapid loading and sliding of MutSα–MutLα recognition complexes at rates much faster than rates of dissociation into solution ($t_{1/2} \propto 0.5$ min). Otherwise, when the hMutSα:substrate ratio was low, substrates could never retain the multiple recognition complexes postulated by the diffusing-recognition-clamp model (Figure 1, upper pathway) long enough to provoke excision. Studies with purified MutSα and MutL proteins (by others) suggest that loading and sliding rates are generally not fast enough. Furthermore, loading of multiple recognition complexes at the same time would be statistically improbable at low hMuSα:DNA ratios. Therefore, the rate of dissociation needs to be fast enough for rapid recycling of recognition complexes, which is not the case. Finally, models in which recognition complexes load, slide, and recycle many times provide no compelling explanation for the strong dependence of excision–initiation rate on mismatch-nick contour distance. Our stoichiometry data appear consistent with two models: loading of single recognition complexes that remain at mismatches (which we favor), or loading of 1–2 complexes that translocate to mismatches along paths already determined by through-space interactions between mismatch-associated and nick-associated proteins.

(II) *Absolute preference for shorter-path 3′–5′ excision in substrates where the 5′–3′ path is only 55% longer*. This observation argues further against models in which multiple MutSα–MutLα recognition complexes load at mismatches, stochastically choose mismatch-nick paths, and move along them until the first-arriving complex automatically triggers excision back along the path just traversed. When path lengths do not differ dramatically, some stochastically loaded complexes traveling the 5′–3′ path should reach the nick first and trigger (processive) longer-path (5′–3′) MMR excision, which was not observed. However, neither outcome (*I*) nor (II) themselves rule out *single* recognition complexes that translocate from mismatches to nicks, then always trigger excision of the shorter (3′–5′) nick-mismatch paths. For example, MutSα•MutLα complexes arriving from *either* (stochastically chosen) direction might form, with nick-associated proteins, the same pre-excision super-complexes. These would then identify appropriate paths for excision—either always favoring 3′–5′ paths, or always favoring shorter paths (always 3′–5′ in our experiments). Alternatively, MutSα–MutLα complexes initially loaded at mismatches might first interact with nick-associated proteins through space and identify appropriate mismatch-nick paths, then move along them to nicks and automatically trigger excision back along the path just traversed.

(III) *Decrease in excision–commitment rate with mismatch-nick distance D as* $D^{-0.43}$. We described above models in which one or two MutSα–MutLα complexes unidirectionally slide from mismatches to nicks, before or after other reaction stages during which appropriate excision paths were identified. Could such compound models explain the observed variation of excision–commitment rate with mismatch-nick contour distance as $D^{-0.43}$, which is not the D^{-1} expected for translocation at a *uniform* rate? Under 'Supplementary Information, Alternative Interpretations of Measurements for hMutSα:DNA Stoichometry and Excision Rates versus Nick-Mismatch Distance', we consider two compound models (i, ii) that assume putative translocating recognition complexes to move at uniform rates. We show neither to be consistent with the $D^{-0.43}$ dependence of excision–initiation rate. Another model (iii) postulates stochastic choice of translocation paths by recognition complexes that move extremely rapidly to nicks. Upon arrival, they form excision super-complexes that identify correct nick-mismatch paths and commit to their excision in a step with rate $\propto D^{-0.43}$. Experiments (by others) suggest MutSα–MutLα translocation rates to be an order of magnitude or so too slow to support this model. Another model (iv) postulates initial through-space interactions with nick-associated proteins that drive rate-limiting translocation of a single recognition complex along (only) the correct path and, by continuing interactions, prevent premature dissociation of the recognition complexes into solution. Arrival of the recognition complex at the nick would automatically and rapidly provoke excision of the correct nick-mismatch path (always the shorter one? always the 3′–5′ path?). Such assisted translocation at a rate $\propto D^{-0.43}$ would be consistent with all our observations. A final model (v) postulates through-space interactions that, without translocation, rapidly trigger a second-phase of identification of the correct nick-mismatch path and commitment to its excision, at a rate $\propto D^{-0.43}$. Such models are considered further later.

(IV) *Failure of mismatched DNA to stimulate in trans excision of nicked homoduplexes*. Mismatch-associated proteins might interact through space to form with nick-associated proteins pre-excision super-complexes whose geometry might immediately dictate 3′–5′ excision. However, we observed 30 nM (non-nicked) mismatched DNA to provoke no detectable excision of 30 nM nicked homoduplex DNA in *trans*. Under 'Supplementary Information, MMR–Protein Interactions Through Space', we estimated the average concentrations of nicks in the presence of mismatches in the same substrate to be (very roughly) 100 nM, on the basis of previous analyses (by others) of DNA cyclization reactions. This estimate predicts a ratio of putative *trans*-provoked to actual *cis*-provoked excision of roughly 0.3. Some *trans* reaction would be detectable even if nicks and mismatches in the *cis* substrates were more than an order of magnitude closer to one another than the cyclization studies might suggest. The absence of *any* detectable excision in *trans* thus

falsifies this simple one-stage model. We note that previous demonstrations of MutS-dependent enhancement of MutL-dependent nicking at hemimethylated d(GATC) sites by mismatched DNA in *trans* (at high non-physiological concentrations of purified proteins) did not address subsequent initiation of excision at these nicks (21,23).

(V) *Apparent competition between (nick/gap)-associated proteins in trans versus cis for interaction with mismatched-associated proteins*. Commitment to mismatch-provoked excision might occur in two stages: initial through-space interactions between mismatch-associated and nick-associated proteins to form excision super-complexes, then identification by them of correct nick-mismatch paths. We showed here (Figure 8) that 30 nM gapped homoduplex plasmid DNA, to which PCNA and RFC are expected to be bound (24), interfered in trans with initiation of 3′–5′ excision of 5 nM test substrate at a nick in cis to a (G/T) mismatch. The concentrations of hPCNA, hRFC, hMutSα, hMutLα and hRPA were expected to exceed the combined concentrations of the competitor and (G/T) test substrate, and hEXOI is expected to interact specifically and strongly with the (G/T) substrate (Figure 7, lanes 2 versus 6). We therefore suggest that gap-associated proteins in *trans* to mismatches compete with nick-associated proteins in *cis* for interactions with mismatch-associated proteins, rather than simply titrating out (a) rate-limiting protein(s). Under 'Supplementary Information, DNA Bending and MMR', the observed 20–40% inhibition in trans is shown to be roughly consistent with the concentration of the nick and the mismatch in the presence of one another, as predicted on the basis of the previously measured value of the Jacobson–Stockmayer cyclization parameter *j*. [Other work (14) also suggests that hEXOI would be preferentially associated with hMutSα bound to the mismatches.] We cannot unequivocally rule out titration of some unknown extract protein by the gapped competitor, or reduction of hPCNA and hRFC to low levels that (while still >5 nM) were insufficient to drive efficient binding to the test substrate. However, this experiment certainly does not falsify two-stage interaction-through-space models. Below we consider explicitly one such a model.

In the two-stage MMR coupling model represented by Equation (1) below, initial activation is followed by identification of the correct nick-mismatch path and initiation of its excision.

$$B \underset{k_{21}}{\overset{k_{12}}{\rightleftharpoons}} C,\ C + E \underset{k_{32}}{\overset{k_{23}}{\rightleftharpoons}} \mathrm{EC} \xrightarrow{k_{34}} P + E. \qquad \mathbf{1}$$

Here *B* is a circular substrate in which separated protein complexes are *bound* to mismatches and nicks and *C* a *coupling* intermediate in which the respective complexes have made productive interactions. EC is the *excision–commitment* super-complex formed by interactions between mismatch-associated and nick-associated proteins and perhaps by recruitment of additional proteins. EC is converted into the excision-committed *product P* by a series of steps subsumed into the single rate constant k_{34}. Equation (1) could describe two-stage models in which: (*a*) the through-space EC super-complex itself determined which of the two immediately adjacent nick-mismatch paths was correct and directly committed to its excision; or (*b*) the EC complex guided translocation of the recognition complex along the correct path to the nick (perhaps at a non-uniform rate), where it then automatically triggered excision back along the path just traveled. Either model might account for the observed dependence of excision commitment on nick-mismatch distance *D*, if the efficiency of an initial rapid through-space equilibrium were *D*-independent and subsequent steps resulted in a $D^{-0.43}$ dependence. We discuss under 'Supplementary Information, DNA Bending and MMR' the direct analogy between reactions describe by Equation (1) and previously analyzed DNA cyclization (25,26). The efficiency of the cyclization reaction turns out to depend on the equilibrium constant for rapid through-space interaction between the two DNA ends, which is in turn directly proportional to the Jacobson–Stockmayer parameter *j*. This parameter, hence the efficiency of the cyclization reaction, is nearly constant for the length range 0.3–1 kbp, because stiffness and length effects balance out (Figure 4S). By *analogy*, if the *only* step in Equation (1) dependent on the mismatch-nick distance *D* were the initial formation of intermediate *C*, then the reaction efficiency would depend on *j*, hence be nearly constant for *D* between 0.23 and 1 kbp, contrary to observation. Thus, in this model steps after initial through-space interactions would have to be responsible for the observed $D^{-0.43}$ dependence. The initial interactions postulated for Equation (1) might involve some or all of the contacts previously demonstrated among MMR and MMR-accessory proteins: PCNA with MSH6 (27–31), PCNA with MLH1 (32), MutLα with MutSα (33–37), ExoI with PCNA, MutLα and MutSα (15,38).

How might proteins interrogate nick-mismatch DNA contours? Modrich has suggested that binding of MutS homologs to mismatches might stimulate MutL-homolog proteins to form long polymers (39), or progressively treadmilling oligomers (40), along nick-mismatch paths. The ability of MutLα to cooperatively form polymers that can interact with two duplexes (41) at once may point to other mechanisms. The incision by hMutLα of exogenous substrates near mismatches [mostly outside pre-existing 3′–5′ nick-mismatch shorter paths (18)] requires both pre-existing nicks and PCNA, as well as mismatches and hMutSα. Such incision by MutLα might help identify 3′–5′ excision paths. The ubiquitous HMGB1 protein, previously implicated in MMR (22,42), might enhance MutLα binding by bending nick-mismatched paths (4,5). HGMB1 can help cyclize linear DNA as short as 60–100 bp (43,44); recent atomic force microscopy shows even such short DNA to be somewhat flexible (45). Conversely, preference of HMGB1 protein for more sharply bent DNA might help distinguish shorter from longer nick-mismatch paths. A number of these mechanisms seem compatible with the $D^{-0.43}$ dependence of excision–commitment rate.

In summary, our observations appear inconsistent with MMR models that invoke movement of multiple recognition complexes along stochastically chosen paths from

mismatches to excision–initiation sites, where they automatically trigger excision along the paths just traveled. Our findings do not falsify two-stage reaction models in which initial activation through space is followed by a distance-dependent process that identifies the correct excision path or translocation models in which recognition proteins are guided to translocate along shorter mismatch-nick paths at rates not uniformly proportional to path length, without premature dissociation into solution; arrival of recognition complexes would then automatically trigger excision back along the paths just traveled.

Quite recently, Pluciennik and Modrich (46), using purified *E. coli* proteins and 6-kbp substrates with single hemi-methylated d(GATC) sites 1024 bp from G/T mismatches, addressed the mechanism by which communication between these two sites activates *E. coli* MutH to nick the unmethylated-d(GATC) strand. They showed interruption of the 1024-bp path by a protein blockade or a double-strand break, respectively, to substantially or completely abolish activation of MutH (dependent on a mismatch, and *E. coli* MutS and MutH). Kolodner *et al.* (47) considered the significance of this finding in a short review. The strong inference is that MutH activation requires communication 'in *cis*' between the mismatch and the hemi-methylated d(GATC) sites. Sliding/translocation of MutS/MutL recognition complexes from mismatches to nicks might accomplish this, but Modrich and Pluciennik did not specify the mechanism of communication. For example, they did not rule out protein polymerization along this path. We note that one alternative mechanism for human MMR proposed above by us, translocation assisted by continuing through-space interaction between the mismatch and excision–initiation sites—would be compatible with the observations of Modrich *et al.* Continued through-space interactions might help direct loading of *E. coli* UvrD helicase in such a way as to move it back towards the mismatch.

However, *E. coli* and eukaryotic MMR now appear to be fundamentally different, and observations made with one system are not necessarily applicable to the other. Notably, a cryptic endonuclease site in the PMS2 subunit of human MutLα (PMS1 in yeast), is essential for MMR. This endonuclease, whose activation requires as well MutSα and a mismatch, and PCNA, RFC and a pre-existing strand interruption, can incise the interrupted strand at any position, with some bias towards sites near but outside the mismatch (18). The new incisions might be used directly by EXOI for 5′–3′ excision and/or mark the ends of 3′–5′ and 5′–3′ excision paths initiated at the pre-existing strand interruptions (see 'Evidence for 3′–5′ rather than 5′–3′ MMR Excision' section in Supplementary Data). The absence of this endonuclease site in *E. coli* MutL may reflect underlying differences in the respective mechanisms. First, one might expect mismatches in newly replicated *E. coli* DNA to usually be closely flanked by hemi-methylated d(GATC) sites on both sides (average distance 128 kbp). Thus, whether MutH is activated at the d(GATC) site that happens to be closer may not be critical. On the other hand, for eukaryotic leading-strand synthesis, the wrong direction from the mismatch leads away from the 3′ OH end at which excision can be initiated. Second, eukaryotic MutLα apparently needs to interact with both mismatch-associated MutSα and pre-existing nick-associated PCNA, then incise the substrate at a point hundreds, or even thousands of base-pairs from the pre-existing nicks (and the mismatch), but always on the pre-existing-nick strand. These requirements seem incompatible with simple sliding/translocation mechanisms.

Finally, we note that sliding along DNA in complex extracts, where it might be bound non-specifically by proteins such as HMGB1, may be much less likely than sliding along naked DNA. Perhaps the same protein–protein interactions that can be achieved only via through-space contacts in complex extracts can be accomplished by sliding/translocation in reconstituted mixtures.

SUPPLEMENTARY DATA

Supplementary Data are available at NAR online.

ACKNOWLEDGEMENTS

We thank the National Cell Culture Center for growth of HeLa cells, and Andrew Buermeyer, Laura Hays, Peter Hoffman, Joyce Lebbink, Stephanie Smith-Roe and Scott Nelson for helpful comments. We thank Guo-Min Li, Myron Goodman, Paul Modrich and Michael Liskay for purified proteins. We thank Ms Tania Porter, Ms JayLene Seeley and Ms Susan Sukontarak for expert preparation of the manuscript. This work was supported by grant ES009848 to J.B.H. from the National Institute of Environmental Health Sciences, NIH, and a grant from the Medical Research Foundation of Oregon. Funding to pay the Open Access publication charges for this article was provided by OSU Foundation.

Conflict of interest statement. None declared.

REFERENCES

1. Kunkel,T.A. and Erie,D.A. (2005) DNA mismatch repair. *Annu. Rev. Biochem.*, **74**, 681–710.
2. Iyer,R.R., Pluciennik,A., Burdett,V. and Modrich,P.L. (2006) DNA mismatch repair: functions and mechanisms. *Chem. Rev.*, **106**, 302–323.
3. Cooper,D.L., Lahue,R.S. and Modrich,P. (1993) Methyl-directed mismatch repair is bidirectional. *J. Biol. Chem.*, **268**, 11823–11829.
4. Grilley,M., Griffith,J. and Modrich,P. (1993) Bidirectional excision in methyl-directed mismatch repair. *J. Biol. Chem.*, **268**, 11830–11837.
5. Viswanathan,M., Burdett,V., Baitinger,C., Modrich,P. and Lovett,S.T. (2001) Redundant exonuclease involvement in Escherichia coli methyl-directed mismatch repair. *J. Biol. Chem.*, **276**, 31053–31058.
6. Fang,W.-H. and Modrich,P. (1993) Human strand-specific mismatch repair occurs by a bidirectional mechanism similar to that of the bacterial reaction. *J. Biol. Chem.*, **268**, 11838–11844.
7. Wang,H. and Hays,J.B. (2002) Mismatch repair in human nuclear extracts: time courses and ATP requirements for kinetically distinguishable steps leading to tightly controlled 5′ to 3′ and aphidicolin-sensitive 3'to 5'mispair-provoked excision. *J. Biol. Chem.*, **277**, 26143–26148.
8. Wang,H. and Hays,J.B. (2003) Mismatch repair in human extracts: effects of internal hairpin structures between mismatches and

excision-initiation nicks on mismatch correction and mismatch-provoked excision. *J. Biol. Chem.*, **278**, 28686–28693.
9. Wang,H. and Hays,J.B. (2002) Mismatch repair in human nuclear extracts: quantitative kinetic analyses of excision of nicked circular mismatched DNA substrates, constructed by a new technique employing synthetic oligonucleotides. *J. Biol. Chem.*, **277**, 26136–26142.
10. Wang,H. and Hays,J.B. (2000) Preparation of mismatched-DNA substrates. *Molec. Biotechnol.*, **15**, 97104.
11. Wang,H. and Hays,J.B. (2006) In Henderson,D.S. (ed.), *DNA Repair Protocols: Mammalian Systems,* Vol. 314, 2nd edn. Humana Press, Totowa, NJ. Humana Press, Totowa, NJ, pp. pp. 345–353.
12. Wang,H. and Hays,J. (2006) *Current Protocols in Toxicology*. John Wiley & Sons, Inc., pp. 3.10.11–13.10.12.
13. Tomer,G., Buermeyer,A.B., Nguyen,M.M. and Liskay,R.M. (2002) Contribution of human mlh1 and pms2 ATPase activities to DNA mismatch repair. *J. Biol. Chem.*, **277**, 21801–21809.
14. Genschel,J. and Modrich,P. (2003) Mechanism of 5'-directed excision in human mismatch repair. *Molec. Cell*, **12**, 1077–1086.
15. Dzantiev,L., Constantin,N., Genschel,J., Iyer,R.R., Burgers,P.M. and Modrich,P. (2004) A defined human system that supports bidirectional mismatch-provoked excision. *Molec. Cell*, **15**, 31–41.
16. Hays,J.B., Hoffman,P.D. and Wang,H. (2005) Discrimination and versatility in mismatch repair. *DNA Repair*, **4**, 1463–1474.
17. Wang,H. and Hays,J.B. (2004) Signaling from DNA mispairs to mismatch-repair excision sites despite intervening blockades. *EMBO J.*, **23**, 2126–2133.
18. Kadyrov,F.A., Dzantiev,L., Constantin,N. and Modrich,P. (2006) Endonucleolytic function of MutLalpha in human mismatch repair. *Cell*, **126**, 297–308.
19. Drummond,J.T., Genschel,J., Wolf,E. and Modrich,P. (1997) *DHFR/MSH3* amplification in methotrexate-resistant cells alters the hMutSa/hMutSa ratio and reduces the efficiency of base-base mismatch repair. *Proc. Natl Acad. Sci. USA*, **94**, 10144–10149.
20. Genschel,J., Bazemore,L.R. and Modrich,P. (2002) Human Exonuclease I is required for 5′ and 3′ mismatch repair. *J. Biol. Chem.*, **277**, 13302–13311.
21. Junop,M.S., Obmolova,G., Rausch,K., Hsieh,P. and Yang,W. (2001) Composite active site of an ABC ATPase: MutS uses ATP to verify mismatch recognition and authorize DNA repair. *Molec. Cell*, **7**, 1–12.
22. Zhang,Y., Yuan,F., Presnell,S.R., Tian,K., Gao,Y., Tomkinson,A.E., Gu,L. and Li,G.M. (2005) Reconstitution of 5'-directed human mismatch repair in a purified system. *Cell*, **122**, 693–705.
23. Schofield,M.J., Brownewell,F.E., Nayak,S., Du,C., Kool,E.T. and Hsieh,P. (2001) The Phe-X-Glu DNA binding motif of MutS. The role of hydrogen bonding in mismatch recognition. *J. Biol. Chem.*, **276**, 45505–45508.
24. Podust,L.M., Podust,V.N., Sogo,J.M. and Hübscher,U. (1995) Mammalian DNA polymerase auxiliary proteins: analysis of replication factor C-catalyzed proliferating cell nuclear antigen loading onto circular double-stranded DNA. *Mol. Cell. Biol.*, **15**, 3072–3081.
25. Shore,D., Langowski,J. and Baldwin,R.L. (1981) DNA flexibility studied by covalent closure of short fragments into circles. *Proc. Natl Acad. Sci. USA*, **78**, 4833–4837.
26. Shore,D. and Baldwin,R.L. (1983) Energetics of DNA twisting. I. Relation between twist and cyclization probability. *J. Mol. Biol.*, **170**, 957–981.
27. Umar,A., Buermeyer,A.B., Simon,J.A., Thomas,D.C., Clark,A.B., Liskay,R.M. and Kunkel,T.A. (1996) Requirement for PCNA in DNA mismatch repair at a step preceding DNA resynthesis. *Cell*, **87**, 65–73.
28. Gu,L., Hong,Y., McCulloch,S., Watanabe,H. and Li,G.M. (1998) ATP-dependent interaction of human mismatch repair proteins and dual role of PCNA in mismatch repair. *Nucleic Acids Res.*, **26**, 1173–1178.
29. Flores-Rozas,H., Clark,D. and Kolodner,R.D. (2000) Proliferating cell nuclear antigen and Msh2p-Msh6p interact to form an active mispair recognition complex. *Nature Genet.*, **26**, 375–378.
30. Clark,A.B., Valle,F., Drotschmann,K., Gary,R.K. and Kunkel,T.A. (2000) Functional interaction of proliferating cell nuclear antigen with MSH2-MSH6 and MSH2-MSH3 complexes. *J. Biol. Chem.*, **275**, 36498–36501.
31. Kleczkowska,H.E., Marra,G., Lettieri,T. and Jiricny,J. (2001) hMSH3 and hMSH6 interact with PCNA and colocalize with it to replication foci. *Genes Dev.*, **15**, 724–736.
32. Lee,S.D. and Alani,E. (2006) Analysis of interactions between mismatch repair initiation factors and the replication processivity factor PCNA. *J. Mol. Biol.*, **355**, 175–184.
33. Blackwell,L.J., Wang,S. and Modrich,P. (2001) DNA chain length dependence of formation and dynamics of hMutS α-hMutL α-heteroduplex complexes. *J. Biol. Chem.*, **276**, 33233–33240.
34. Mendillo,M.L., Mazur,D.J. and Kolodner,R.D. (2005) Analysis of the interaction between the Saccharomyces cerevisiae MSH2-MSH6 and MLH1-PMS1 complexes with DNA using a reversible DNA end blocking system. *J. Biol. Chem.*, **80**, 22245–22257.
35. Habraken,Y., Sung,P., Prakash,L. and Prakash,S. (1998) ATP-dependent assembly of a ternary complex consisting of a DNA mismatch and the yeast MSH2-MSH6 and MLH-PMS1 protein compexes. *J. Biol. Chem.*, **273**, 9837–9841.
36. Bowers,J., Tran,P.T., Liskay,R.M. and Alani,E. (2000) Analysis of yeast MSH2-MSH6 suggests that the initiation of mismatch repair can be separated into discrete steps. *J. Mol. Biol.*, **302**, 327–338.
37. Raschle,M., Dufner,P., Marra,G. and Jiricny,J. (2002) Mutations within the hMLH1 and hPMS2 subunits of the human MutLalpha mismatch repair factor affect its ATPase activity, but not its ability to interact with hMutSalpha. *J. Biol. Chem.*, **277**, 21810–21820.
38. Schmutte,C., Sadoff,M.M., Shim,K.-S., Acharya,S. and Fishel,R. (2001) The interaction of DNA mismatch repair proteins with human exonuclease I. *J. Biol. Chem.*, **276**, 33011–33018.
39. Modrich,P. (1987) DNA mismatch correction. *Annu. Rev. Biochem.*, **56**, 435–466.
40. Iyer,R.R., Pluciennik,A., Burdett,V. and Modrich,P.L. (2006) DNA mismatch repair: functions and mechanisms. *Chem. Rev.*, **106**, 302–323.
41. Hall,M.C., Wang,H., Erie,D.A. and Kunkel,T.A. (2001) High affinity cooperative DNA binding by the yeast Mlh1-Pms1 heterodimer. *J. Mol. Biol.*, **312**, 637–647.
42. Yuan,F., Gu,L., Guo,S., Wang,C. and Li,G.M. (2004) Evidence for involvement of HMGB1 protein in human DNA mismatch repair. *J. Biol. Chem.*, **279**, 20935–20940.
43. Pil,P.M., Chow,C.S. and Lippard,S.J. (1993) High-mobility-group 1 protein mediates DNA bending as determined by ring closures. *Proc. Natl Acad. Sci. USA*, **90**, 9465–9469.
44. Stros,M. (1998) DNA bending by the chromosomal protein HMG1 and its high mobility group box domains. Effect of flanking sequences. *J. Biol. Chem.*, **273**, 10355–10361.
45. Wiggins,P.A., Van Der Heijden,T., Moreno-Herrero,F., Spakowitz,A., Phillips,R., Widom,J., Dekker,C. and Nelson,P.C. (2006) High flexibility of DNA on short length scales probed by atomic force microscopy. *Nature Nanotechnol.*, **1**, 137–141.
46. Pluciennik,A. and Modrich,P. (2007) Protein roadblocks and helix discontinuities are barriers to the initiation of mismatch repair. *Proc. Natl Acad. Sci. USA*, **104**, 12709–12713.
47. Kolodner,R.D., Mendillo,M.L. and Putnam,C.D. (2007) Coupling distant sites in DNA during DNA mismatch repair. *Proc. Natl Acad. Sci. USA*, **104**, 12953–12954.